Photosynth Res
DOI 10.1007/s11120-014-9990-y

REGULAR PAPER

On destabilization of the Fenna–Matthews–Olson complex of *Chlorobaculum tepidum*

Adam Kell · Khem Acharya · Robert E. Blankenship · Ryszard Jankowiak

Received: 13 November 2013 / Accepted: 17 February 2014

Abstract The Fenna–Matthews–Olson (FMO) complex from the green sulfur bacterium *Chlorobaculum tepidum* was studied with respect to its stability. We provide a critical assessment of published and recently measured optical spectra. FMO complexes were found to destabilize over time producing spectral shifts, with destabilized samples having significantly higher hole-burning efficiencies; indicating a remodeled protein energy landscape. Observed correlated peak shifts near 825 and 815 nm suggest possible correlated (protein) fluctuations. It is proposed that the value of 35 cm^{-1} widely used for reorganization energy (E_λ), which has important implications for the contributions to the coherence rate (Kreisbeck and Kramer 3:2828–2833, 2012), in various modeling studies of two-dimensional electronic spectra is overestimated. We demonstrate that the value of E_λ is most likely about 15–22 cm^{-1} and suggest that spectra reported in the literature (often measured on different FMO samples) exhibit varied peak positions due to different purification/isolation procedures or destabilization effects.

Keywords FMO · Light harvesting · Photosynthesis · Spectral hole burning

A. Kell · K. Acharya · R. Jankowiak
Department of Chemistry, Kansas State University, Manhattan, KS 66506, USA

R. E. Blankenship
Departments of Chemistry and Biology, Washington University in St. Louis, St. Louis, MO 63130, USA

R. Jankowiak (✉)
Department of Physics, Kansas State University, Manhattan, KS 66506, USA
e-mail: ryszard@ksu.edu

Abbreviations

(BChl)	Bacteriochlorophyll
(EET)	Excitation energy transfer
(FMO)	Fenna–Matthews–Olson
(HB)	Hole-burning
(RCs)	Reaction centers
(E_λ)	Reorganization energy

Introduction

Green sulfur bacteria contain a bacteriochlorophyll (BChl) *a* binding antenna complex called the Fenna–Matthews–Olson (FMO) protein (Milder et al. 2010; Olson 2004; Olson and Romano 1962). FMO connects the chlorosome to the reaction center (RC) in the cytoplasmic membrane and functionally forms a bridge to transfer excitation energy. The structure of FMO from *Chlorobaculum* (*C.*) *tepidum* has been determined by X-ray diffraction to be a trimer with C_3-symmetry containing seven BChl *a* pigments per monomer (Camara-Artigas et al. 2003). A more recent model of the crystal structure includes an eighth pigment in a similar binding pocket as observed for *Prosthecochloris aestuarii* (Tronrud et al. 2009), while mass spectrometry data revealed BChl *a* 8 in *C. tepidum* with partial occupancy (Wen et al. 2011). Currently, only a single monomer is taken into account in simulations of optical spectra and, due to an assumed low occupancy or absence in isolated complexes, the eighth pigment is often neglected (Adolphs and Renger 2006; Cho et al. 2005; Vlaming and Silbey 2012). Even so, different sets of electronic site energies used in theoretical studies lead to differences in the reported transfer dynamics (Adolphs and Renger 2006; Cho et al. 2005; Vlaming and Silbey 2012),

Published online: 01 March 2014

which may cause additional suppression or enhancement of oscillations (i.e., long-lived quantum coherences). This work will address differences arising in FMO sample preparations that, at least in part, contribute to the vast amount of site energies available and the absence of a consensus about the excitonic structure in the literature.

To study stability and intactness of various FMO samples from *C. tepidum* we use absorption, emission, and hole-burning (HB) spectroscopies. HB relies on differences observed in the absorption spectrum of a low-temperature system after narrow-band laser excitation. In general, if a pigment molecule (in resonance with the laser) undergoes a photochemical reaction, it ceases to absorb at its original wavelength/frequency and one speaks of photochemical HB (PHB). In the case of non-photochemical HB (NPHB) the pigment molecule does not undergo a chemical reaction, but its immediate environment experiences some rearrangement; for more details see (Jankowiak et al. 2011, 2012). Both PHB and NPHB result in the formation of persistent holes, meaning the holes are preserved after the initial excitation is turned off, as long as low temperature is maintained. In either case, the HB spectrum is obtained as the difference between the measured absorption spectrum before and after laser excitation. Both resonant and nonresonant holes can be obtained (Jankowiak et al. 2011). In this work, we focus on nonresonant (persistent) holes formed by downward energy relaxation along the "excitonic energy ladder" within the trimer; such holes reveal the shape of the lowest energy excitonic state from which emission occurs. A theoretical description of the excitonic structure of the entire trimer and excitation energy transfer (EET) processes will be discussed elsewhere.

Materials and methods

Fenna–Matthews–Olson complexes were prepared as described previously (Wen et al. 2009, 2010) with a 50 mM Tris–HCl buffer and stored in a freezer ($\sim$0 °C). A glass-forming solution of glycerol and ethylene glycol (55:45 v/v) was added to all samples (OD_{825} was 0.2–0.4). Details about the experimental setup were described elsewhere (Feng et al. 2011). Briefly, absorption and HB spectra were measured by a Bruker HR125 Fourier transform spectrometer. For all absorption and HB spectra, a spectral resolution of 4 cm^{-1} was used. Fluorescence spectra were collected, with a resolution of 0.1 nm, by a Princeton Instruments Acton SP-2300 spectrograph equipped with a back-illuminated CCD camera (PI Acton Spec10, 1,340×400). The laser source (λ = 496.5 nm) for fluorescence and (nonresonant) HB spectra was produced by a Coherent Innova 200 argon ion laser. Laser power was set by a continuously adjustable neutral density filter. Experiments were performed at 5 K inside either a Janis 8-DT Super Vari-Temp liquid helium cryostat or an Oxford Instruments Optistat CF2 cryostat. Sample temperature was read and controlled with a Lakeshore Cryotronic model 330 or Mercury iTC temperature controller for the former and latter cryostats, respectively.

Results and discussion

Absorption and HB spectra

An adequate theoretical description of the excitonic structure and EET dynamics in FMO complexes requires data obtained for intact protein complexes. However, the band positions (and peak intensity distribution) of low-temperature optical spectra of FMO from *C. tepidum* reported in the literature vary (Cho et al. 2005; Rätsep and Freiberg 2007; Vulto et al. 1998), although the changes were admittedly rather small ($\Delta\lambda \leq 1$ nm). The latter, however, does not mean that small shifts of the electronic transitions do not affect the dynamics of the studied protein system, e.g., the HB yield. For consistency, the three resolvable peaks will be referred to by the peak positions of the most red shifted spectrum: 826, 816, and 805 nm peaks. It was observed that some peaks in the absorption spectra shifted continuously over time, even though samples were kept in a freezer and in the absence of light. That is, peak positions shifted to higher frequency with time. However, it was also found that some fresh samples had blue-shifted absorption peaks; indicating that the peak position also depends on the sample preparation procedures. These data present a constraint on the interpretation of FMO optical spectra and their underlying electronic structure.

To illustrate this problem, we present low-temperature (5 K) absorption, fluorescence, and HB spectra obtained for intact samples, whose 826 nm band positions are compared with data obtained for destabilized samples and previously reported results. As an example, Fig. 1a shows absorption and nonresonant HB spectra for samples measured in 2009 (curve a) and 2012 (curve b). After 1 year, the sample measured in 2009 had a shifted absorption spectrum similar to the fresh 2012 sample shown in Fig. 1a. Thus, the FMO samples can destabilize over time or by preparation procedures but either way results in similar blue-shifted absorption spectra. The observed blue shift in the Q_y absorption region from the 2009 sample (curve a) to the 2012 sample (curve b in Fig. 1a) is $\sim$1 nm (15 cm^{-1}) for both the 826 and 816 nm peaks, which indicates the changes are occurring mainly to the two lowest energy absorption bands, as shown by the difference spectrum (c = b–a; red curve). Based on excitonic calculations reported previously (Adolphs and Renger 2006;

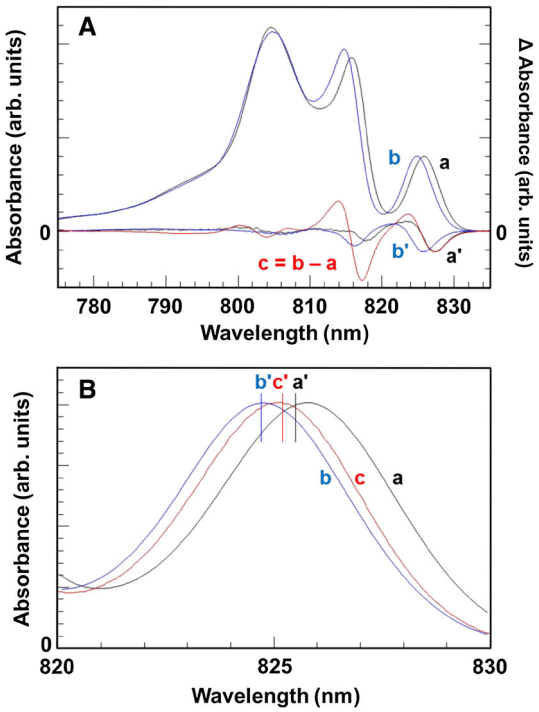

Fig. 1 *Frame A*: *Curves a* and *b* correspond to the absorption spectra obtained for FMO samples measured in 2009 and 2012, respectively. The difference between spectra is shown as curve c (c = b–a). Curves *a*′ and *b*′ are the saturated nonresonant HB spectra (λ_B = 496.5 nm) obtained for *curves a* and *b*, respectively. The spectra are normalized to the low-energy band/hole. *Frame B*: The two 825 nm bands for FMO samples shown above (*curves a* and *b*) as well as an absorption band measured in 2010 (*curve c*). The *vertical lines* mark the peak positions of 825 nm bands reported in the literature (see text for details)

Cho et al. 2005; Vlaming and Silbey 2012; Vulto et al. 1998), this spectral region is mostly contributed to by the two lowest energy excitonic states (vide infra), with some contribution from the third lowest state also.

The lowest energy bands in the nonresonant holes shown in Fig. 1 (curves a′ and b′) correspond to the lowest energy trap states of the FMO samples represented by absorption spectra a and b, respectively, since the NPHB rate is much smaller than both fluorescence and EET rates. Therefore, the shape of the "nonresonant hole origin" is nearly identical to the shape of the emission origin spectrum (Jankowiak et al. 2011; unpublished work). The higher energy bands observed in spectra a′ and b′ in Fig. 1a are due to modified excitonic interactions when HB occurs in the lowest energy state of the excitonically coupled system. However, to explain the shape of emission and nonresonant HB spectra of FMO complexes, a downward uncorrelated EET between FMO trimer subunits has to be taken into account; however, this, as well as the description of the excitonic structure of the entire FMO trimer, is beyond the scope of this manuscript and will be discussed elsewhere.

Frame B in Fig. 1 shows the low-energy bands of FMO (*C. tepidum*) samples measured at different times compared to peak positions reported in the literature (see the vertical lines, which mark the peak positions of 826 nm bands reported in the literature, i.e., 825.5 nm (Rätsep and Freiberg 2007), 824.7 nm (Vulto et al. 1998) and 825.2 nm (Cho et al. 2005) for lines a–c, respectively). Clearly, the experimental curves from this work accurately approximate the range of 826 nm band positions reported in the literature. The similar shifts of both the 826 and 816 nm bands indicate the possibility of spatially correlated environmental fluctuations. From excitonic calculations, the pigments contributing to these two bands are BChl *a* 3–5 and 7 (Adolphs and Renger 2006; Cho et al. 2005; Vlaming and Silbey 2012; Vulto et al. 1998); all of which are likely influenced by the motions of the protein α-helix 5 (Müh et al. 2007). Also, molecular dynamics simulations have shown correlations between the dipole couplings V_{45} and V_{57} (where V_{ij} is the coupling constant between pigments i and j) (Olbrich et al. 2011). A correlation of energy shifts could contribute to a short dephasing time (Caycedo-Soler et al. 2012) and subsequent oscillations between the low-energy exciton states 1 and 2 (Vlaming and Silbey 2012).

For nonresonant HB spectra shown in Fig. 2, a burn frequency of 496.5 nm is used, and the lowest energy hole corresponds to the lowest exciton state. Figure 2 shows the development of holes under increasing fluence ($f = It$; where I is laser intensity and t is burn time) until saturation for samples measured in 2009 and 2012 (see Fig. 1, curves a and b, respectively). The lowest energy hole position for the most intact FMO sample is 827.4 nm. The HB spectra in Fig. 2a are red shifted relative to the position of the corresponding steady-state absorption bands due to the presence of a relatively slow EET between the lowest energy states (mostly localized on BChl *a* 3) of the monomers of the trimer (unpublished work).

The destabilized FMO (2012 sample) has blue-shifted holes, and in contrast to data shown in Fig. 2 (frame A) the hole position (at 826.1 nm for low fluence, shallow hole) shifts to the blue as a function of fluence. That is, in this case the hole position is fluence dependent. This shift (~0.4 nm, relative to the low fluence hole) indicates that the blue-shifted absorption spectrum is likely a mixture of intact and destabilized FMO complexes. A blue shift also occurs in the 816 nm hole, but is half (0.2 nm) that of the low-energy hole. Thus, the overall blue shift of both saturated holes (deepest holes of the 816 and 826 nm bands, curve a′) is 1.7 nm when compared to the saturated hole positions of the 2009 sample (curve a, Fig. 2a); showing, as did the corresponding absorption spectrum, a conserved shift between these two states. The latter suggests that more efficient bleaching occurs in the destabilized FMO sample. Since the intact FMO sample (measured in 2009)

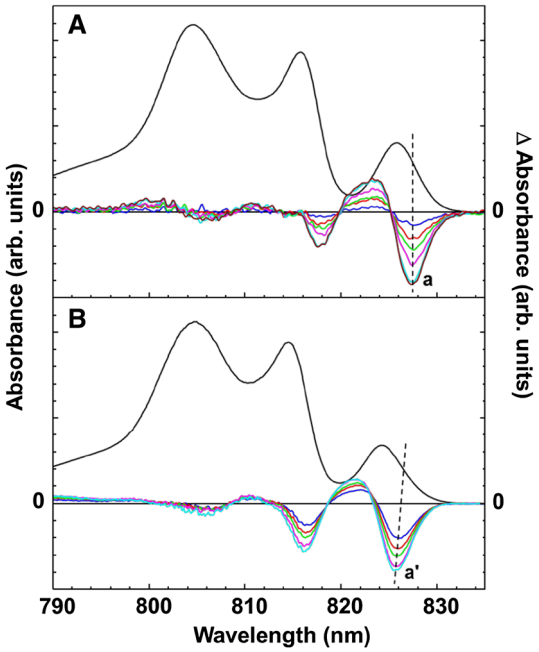

Fig. 2 Absorption spectra and fluence dependent nonresonant HB spectra obtained with a burn wavelength of 496.5 nm. *Dashed lines* are included to guide the eye along the evolving hole position. *Frame A*: Spectra for intact samples. Saturated hole (*curve a*) is located at 827.4 nm and all HB spectra are multiplied by 40. *Frame B*: Spectra for destabilized samples. Saturated hole (*curve a′*) is located at 825.7 nm and HB spectra are multiplied by 4

does not show any noticeable shift in the position of the low-energy hole over the course of burning, this suggests that the preparation is free of destabilized complexes. Interestingly, an absorption band at 826 nm has been observed in the FMO–RC complex and attributed solely to FMO absorption (Francke et al. 1996) in agreement with our observations. In the FMO–RC preparations, pigments contributing to the lowest energy band (i.e., mainly BChl *a* 3) should not be destabilized due to binding of the RC. As such, this supports our assignment that intact complexes have a low-energy absorption band near 826 nm.

To measure the HB efficiency of a system, the percent hole depth (defined for a specific wavelength as the ratio of absorbance change due to HB and original "preburn" absorbance) versus fluence is plotted for each hole burned. The resulting plot for three FMO samples with slightly different 826 nm band positions is shown in Fig. 3. The destabilized sample (with the most blue shifted absorption spectrum) exhibits the largest relative HB efficiency; an effect that has also been reported previously for mixtures of CP47 photosynthetic complexes (Neupane et al. 2010). This change in HB efficiency clearly indicates modified protein landscape tiers that are directly probed by HB spectroscopy. Thus, it cannot be excluded that the theoretical description of experimental data generated for FMO samples with contributions from destabilized proteins could also lead to a slightly modified excitonic structure and, in particular, modified EET dynamics. It appears that even though the sample measured in 2010 (from a different batch) has a blue-shifted 826 nm band, the HB efficiency would indicate that this sample is still mainly contributed to by intact FMO complexes. Thus, the observed differences in shifts may not only be caused by destabilization but also by slightly different pH values, which are difficult to control. That is, it cannot be excluded that the net protein charge near low-energy pigments could change, leading to modified hydrophobic interactions (Hofmann et al. 2013); see also data shown in Figs. 3 and 4.

To assess the contributions of intact and destabilized complexes measured for samples from the same batch, a simple spectral subtraction method was used. The analysis of the absorption (curve b) and HB spectrum (curve b) measured in 2012, shown in Fig. 4, suggests possible contributions from intact (curve a) and destabilized (curve c) FMO proteins. The spectra measured in 2009 represent intact samples, while curves c = b–a and $c' = b'–a'$ were obtained by subtraction after the corresponding spectra were normalized at the low-energy side of the 826 nm band. Curve c′ shows the destabilized complexes are the main contributors to the saturated hole, as suggested above, being consistent with the much higher HB yield observed for blue-shifted samples. We did not attempt to deconvolve emission spectra, as the fluorescence quantum efficiency of intact and destabilized complexes is unknown.

It is not clear, however, by what mechanism this destabilization occurs, especially that similar blue shifts in peak position of the 826 nm band have been produced by oxidation with potassium ferricyanide and reduction with sodium dithionite (data not shown). Similar effects, though more pronounced due to higher concentrations, to those reported by Bina and Blankenship (2013) were observed in the 5 K lowest energy absorption. That is, the band shifts to 824.7 nm after the sample is treated with potassium ferricyanide; the same wavelength as the most destabilized sample found in both our data and the literature absorption spectra (Vulto et al. 1998; Francke et al. 1996). Another possible mechanism, as eluded to above, includes changes to pH of the Tris–HCl buffer solution.

Reorganization and site energies

Figure 5 shows that the low-energy absorption and emission peaks measured in 2009 (frame A) and 2012 (frame B) shift by the same amount ($\sim$1 nm), which leads to conservation of the Stokes shift, and subsequently, the reorganization energy (E_λ). For weak electron–phonon coupling, E_λ can be approximated as half of the Stokes shift, leading to a E_λ of $\sim$11 cm^{-1} from the experimental Stokes shift of $\sim$22 cm^{-1}. The value of E_λ appears to be independent of

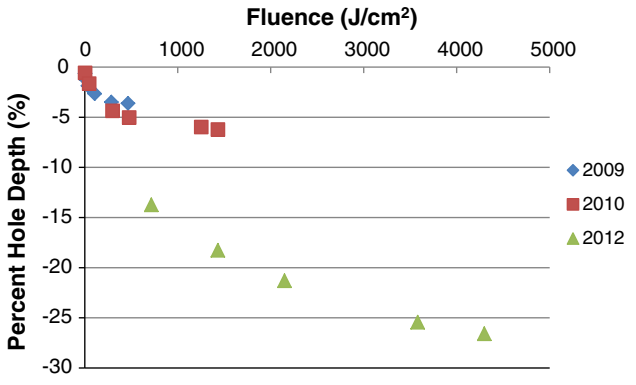

Fig. 3 *Percent hole-depth* plotted as a function of fluence (in J/cm^2). *Blue diamonds* correspond to the most intact FMO complex, while *red squares* and *green triangles* represent complexes measured in 2010 and 2012, respectively

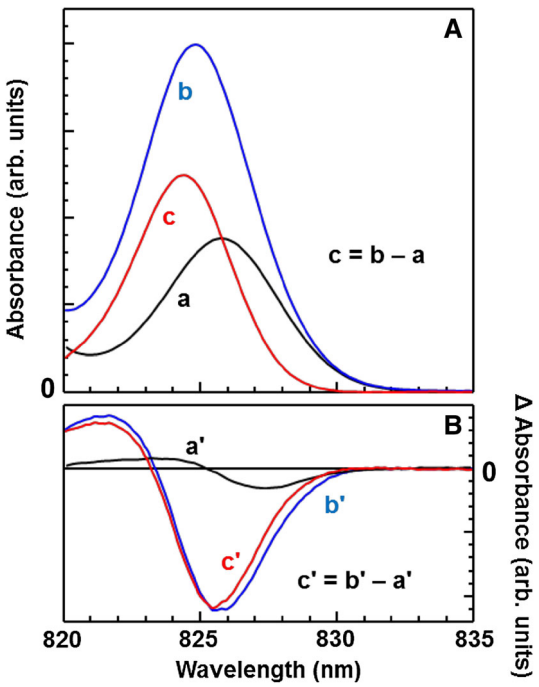

Fig. 4 *Frame A*: 825 nm bands for 2009 measured sample (intact sample; *curve a*) and sample measured in 2012 (destabilized preparation; *curve b*) normalized at the low-energy absorption wing. *Curve c* corresponds to the difference spectrum (c = b–a), assigned as the absorption of destabilized proteins. *Frame B*: Saturated nonresonant holes ($\lambda_B = 496.5$ nm) for the 2009 (*curve a′*) and 2012 (*curve b′*) samples normalized at the low-energy side of the nonresonant hole. *Curve c′* is the difference spectrum (c′ = b′–a′) assigned to the bleach from destabilized complexes. Note the significant difference in HB efficiency

sample age/preparation; however, comparing spectra from different batches, experiments and/or laboratories can lead to overestimated values of E_λ. This is illustrated in frame C of Fig. 5 where the absorption spectrum (curve 2 from frame

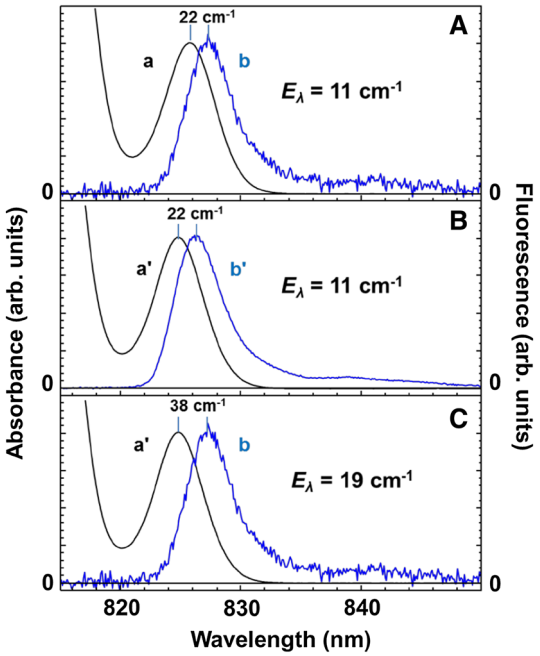

Fig. 5 *Frame A*: Absorption (*curve a*) and emission (*curve b*) spectra obtained for the intact (2009) sample. *Frame B*: Absorption (*curve a′*) and emission (*curve b′*) obtained for the destabilized (2012) sample. In both *frames* the Stokes shift is conserved (see main text for details). *Frame C*: Absorption (*curve a′*) and emission (*curve b*) from frames *A* and *B*, showing that a comparison of spectra from different experiments leads to an incorrect E_λ value

B) is plotted with the emission spectrum (curve 2 from frame A). This proves that comparison of spectra from different experiments can lead to incorrect conclusions about E_λ. Therefore, care must be taken to assess the quality of samples when comparing data.

Regarding the value of E_λ, we note that this parameter can also be calculated from the spectral density (i.e., the weighted one-phonon profile) as

$$E_\lambda = \hbar \int_0^\infty \omega J(\omega) d\omega. \quad (1)$$

However, the values can be highly dependent on the functional choice of the spectral density (Kell et al. 2013) and scale linearly with the Huang–Rhys factor S, which for various FMO complexes ranges from 0.3 to 0.5 in the literature (Adolphs and Renger 2006; Johnson and Small 1991; Rätsep and Freiberg 2007; Wendling et al. 2000). For completeness, Fig. 6 shows the experimental delta fluorescence line-narrowed (ΔFLN) spectrum (Rätsep and Freiberg 2007) compared to the single-site spectrum calculated using a lognormal spectral density (Kell et al. 2013). From this spectral density and Eq. 1 E_λ ranges from 14.6 to 24.3 cm^{-1} for $S = 0.3$–0.5. In a similar manner, the shape of the spectral density can be roughly approximated from

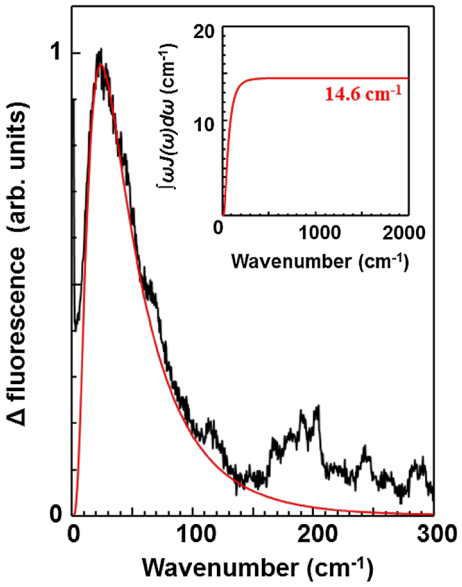

Fig. 6 Experimental ΔFLN spectrum of Rätsep and Freiberg (2007) (*black noisy curve*, $\omega_{ex} = 12090\ cm^{-1}$) compared to the single-site spectrum calculated with the lognormal spectral density of Kell et al. (2013) (*red curve*). The *inset* shows the integral of $\omega J(\omega)$ assuming the Huang–Rhys factor $S = 0.3$

fits of the pseudo-phonon sideband hole (PSBH) found in resonant HB spectra. Calculating E_λ from simplistic fits to the pseudo-PSBH of FMO (data not shown) leads to values of 18.0–30.0 cm^{-1} for the same S values as above. All of the above suggests that the true value of E_λ is likely somewhere in the range of 15–25 cm^{-1}. While the experimental value derived from the Stokes shift is likely underestimated, it appears the often-used value of 35 cm^{-1} (for example in Cho et al. 2005; Ishizaki and Fleming 2009; Pachón and Brumer 2011; Ritschel et al. 2011) is overestimated. This value was derived from fitting a partly destabilized absorption spectrum (lowest energy band of 825.2 nm) using an Ohmic spectral density. It should be noted that often when the overdamped Brownian oscillator spectral density is used for FMO calculations (with E_λ = 35 cm^{-1}), the definition for E_λ includes a π term; meaning the values calculated in this work should be divided by π in order to be directly comparable.

Many sets of site energies listed in the literature are found from fits of optical spectra (Milder et al. 2010, and references therein), although some attempts have been made to elucidate site energies from calculations based on the crystal structure (Adolphs and Renger 2006; Adolphs et al. 2008; Müh et al. 2007). While comparisons would be easily accomplished if the entire absorption spectra shifted in concert, as seen in Fig. 1 this is not the case as the 805 nm band, contributed to by several pigments, never appears to shift. Thus, not all sets of site energies are directly comparable even based on absorption spectra alone. However, as seen in Fig. 5, comparison of absorption and emission spectra measured in different experiments (and/or for samples) can also lead to erroneous conclusions.

Regarding site energies of FMO pigments, the values of Adolphs and Renger (2006) are often used when simulating 2D electronic spectra cross peak oscillations (Christensson et al. 2012; Kreisbeck et al. 2013) and exciton populations (Ishizaki and Fleming 2009; Nalbach et al. 2011). The site energies, specifically for *C. tepdium*, were derived from fits to the linear optical spectra of Vulto et al. (1998), the absorption of which has a very blue shifted 826 nm band (824.7 nm). These parameters cannot fit all of the spectra presented in this work, i.e., absorption for samples measured in 2009 and 2010. As mentioned above, the calculated absorption spectrum from which $E_\lambda = 35\ cm^{-1}$ was derived (Cho et al. 2005) also had a blue-shifted absorption peak and this sample was most likely a mixture of intact and destabilized samples, possibly exhibiting modified excitonic structure and EET dynamics. In fact, none of the published site energies for FMO (*C. tepidum*) can describe simultaneously absorption, emission, CD, LD, persistent, and transient HB spectra, suggesting that proper site energies have not been established as yet (unpublished data).

Conclusions

Based on our data, the low-energy absorption bands near 825 and 815 nm reported in the literature (Cho et al. 2005; Rätsep and Freiberg 2007; Vulto et al. 1998) likely correspond to partly destabilized samples, which, if used in excitonic calculations, could lead to different parameter sets that should not be directly comparable to each other; that is, each set of site energies is dependent on sample preparation. Conserved shifts between absorption bands at 826 and 816 nm point toward correlated effects caused by the protein environment. Such effects have been shown theoretically to decrease the transfer rate to the lowest energy state and preserve coherence (Bhattacharyya and Sebastian 2013; Sarovar et al. 2011). Besides discrepancies in E_λ values used in the modeling of optical spectra for FMO (*C. tepidum*), the apparent peak shifts can also lead to a range of pigment site energies, which are important input parameters into energy transfer and lineshape calculations for excitonically coupled systems. Consideration of the sample preparation procedures when modeling optical spectra of FMO is critical for correct interpretation of the excitonic structure for both isolated proteins and complexes in vivo.

Acknowledgments This work was supported by the Chemical Sciences, Geosciences and Biosciences Division, Office of Basic Energy Sciences, Office of Science, U.S. Department of Energy (Grant DE-FG02-11ER16281 to R.J). Authors are thankful to Mike Reppert (The University of Chicago) and Dr. Valter Zazubovich (Concordia University) for fruitful discussions at the early stage of

this work. FMO complexes were kindly provided by Dr. Jianzhong Wen (Washington University in St. Louis).

References

Adolphs J, Renger T (2006) How proteins trigger excitation energy transfer in the FMO complex of green sulfur bacteria. Biophys J 91:2778–2797

Adolphs J, Müh F, Madjet ME, Renger T (2008) Calculation of pigment transition energies in the FMO protein. Photosynth Res 95:197–209

Bhattacharyya P, Sebastian KL (2013) Adiabatic eigenfunction-based approach for coherent excitation transfer: an almost analytical treatment of the Fenna–Matthews–Olson complex. Phys Rev E 87:062712

Bina D, Blankenship RE (2013) Chemical oxidation of the FMO antenna protein from *Chlorobaculum tepidum*. Photosynth Res 116:11–19

Camara-Artigas A, Blankenship RE, Allen JP (2003) The structure of the FMO protein from *Chlorobium tepidum* at 2.2 Å resolution. Photosynth Res 75:49–55

Caycedo-Soler F, Chin AW, Almeida J, Huelga SF, Plenio MB (2012) The nature of the low energy band of the Fenna–Matthews–Olson complex: vibronic signatures. J Chem Phys 136:155102

Cho M, Vaswani HM, Brixner T, Stenger J, Fleming GR (2005) Exciton analysis in 2D electronic spectroscopy. J Phys Chem B 109:10542–10556

Christensson N, Kauffmann HF, Pullerits T, Mančal T (2012) Origin of long-lived coherences in light-harvesting complexes. J Phys Chem B 116:7449–7454

Feng X, Neupane B, Acharya K, Zazubovich V, Picorel R, Seibert M, Jankowiak R (2011) Spectroscopic study of the CP43 complex and the PSI-CP43 supercomplex of the cyanobacterium *Synechocystis* PCC 6803. J Phys Chem B 115:13339–13349

Francke C, Amesz J (1997) Isolation and pigment composition of the antenna system of four species of green sulfur bacteria. Photosynth Res 52:137–146

Francke C, Otte SCM, Miller M, Amesz J, Olson JM (1996) Energy transfer from carotenoid and FMO-protein in subcellular preparations from green sulfur bacteria. Spectroscopic characterization of an FMO-reaction center core complex at low temperature. Photosynth Res 50:71–77

Hofmann H, Nettles D, Schuler B (2013) Single-molecule spectroscopy of the unexpected collapse of an unfolded protein at low pH. J Chem Phys 139:121930

Ishizaki A, Fleming GR (2009) Theoretical examination of quantum coherence in a photosynthetic system at physiological temperature. Proc Natl Acad Sci USA 106:17255–17260

Jankowiak R (2012) Probing electron-transfer times in photosynthetic reaction centers by hole-burning spectroscopy. J Phys Chem Lett 3:1684–1694

Jankowiak R, Reppert M, Zazubovich V, Pieper J, Reinot T (2011) Site selective and single complex laser-based spectroscopies: a window on excited state electronic structure, excitation energy transfer, and electron–phonon coupling of selected photosynthetic complexes. Chem Rev 111:4546–4598

Johnson SG, Small GJ (1991) Excited-state structure and energy-transfer dynamics of the bacteriochlorophyll *a* antenna complex from *Prosthecochloris aestuarii*. J Phys Chem 95:471–479

Kell A, Feng X, Reppert M, Jankowiak R (2013) On the shape of the phonon spectral density in photosynthetic complexes. J Phys Chem B 117:7317–7323

Kreisbeck C, Kramer T (2012) Long-lived electronic coherence in dissipative exciton dynamics of light-harvesting complexes. J Phys Chem Lett 3:2828–2833

Kreisbeck C, Kramer T, Aspuru-Guzik A (2013) Disentangling electronic and vibronic coherences in two-dimensional echo spectra. J Phys Chem B 117:9380–9385

Olson JM (2004) The FMO protein. Photosynth Res 80:181–187

Olson JM, Romano CA (1962) A new chlorophyll from green bacteria. Biochim Biophys Acta 59:726–728

Milder MTW, Brüggemann B, van Grondelle R, Herek JL (2010) Revisiting the optical properties of the FMO protein. Photosynth Res 104:257–274

Müh F, Madjet ME, Adolphs J, Abdurahaman A, Rabenstein B, Ishikita H, Knapp E, Renger T (2007) α-Helices direct excitation energy flow in the Fenna–Matthews–Olson protein. Proc Natl Acad Sci USA 104:16862–16867

Nalbach P, Braun D, Thorwart M (2011) Exciton transfer dynamics and quantumness of energy transfer in the Fenna–Matthews–Olson complex. Phys Rev E 84:041926

Neupane B, Dang NC, Acharya K, Reppert M, Zazubovich V, Picorel R, Seibert M, Jankowiak R (2010) Insight into the electronic structure of the CP47 antenna protein complex of photosystem II: hole burning and fluorescence study. J Am Chem Soc 132:4214–4229

Olbrich C, Strmüpfer J, Schulten K, Kleinekathöfer U (2011) Quest for spatially correlated fluctuations in the FMO light-harvesting complex. J Phys Chem B 115:758–764

Pachón LA, Brumer P (2011) Physical basis for long-lived electronic coherence in photosynthetic light-harvesting systems. J Phys Chem Lett 2:2732–2778

Rätsep M, Freiberg A (2007) Electron–phonon and vibronic couplings in the FMO bacteriochlorophyll *a* antenna complex studied by difference fluorescence line narrowing. J Lumin 127:251–259

Ritschel G, Roden J, Strunz WT, Aspuru-Guzik A, Eisfield A (2011) Absence of quantum oscillations and dependence on site energies in electronic excitation transfer in the Fenna–Matthews–Olson trimer. J Phys Chem Lett 2:2912–2917

Sarovar M, Cheng Y-C, Whaley KB (2011) Environmental correlation effects on excitation energy transfer in photosynthetic light harvesting. Phys Rev E 83:011906

Tronrud DE, Wen J, Gay L, Blankenship RE (2009) The structural basis for the difference in absorbance spectra for the FMO antenna protein from various green sulfur bacteria. Photosynth Res 100:79–87

Vlaming SM, Silbey RJ (2012) Correlated intermolecular coupling fluctuations in photosynthetic complexes. J Chem Phys 136: 055102

Vulto SIE, de Baat MA, Louwe RJW, Permentier HP, Neef T, Miller M, van Amerongen H, Aartsma TJ (1998) Exciton simulations of optical spectra of the FMO complex from the green sulfur bacterium *Chlorobium tepidum* at 6 K. J Phys Chem B 102:9577–9582

Wen J, Zhang H, Gross ML, Blankenship RE (2009) Membrane orientation of the FMO antenna protein from *Chlorobaculum tepidum* as determined by mass spectrometry-based footprinting. Proc Natl Acad Sci USA 106:6134–6139

Wen J, Harada J, Buyle K, Yuan K, Tamiaki H, Oh-Oka H, Loomis RA, Blankenship RE (2010) Characterization of an FMO variant of *Chlorobaculum tepidum* carrying bacteriochlorophyll *a* esterified by geranylgeraniol. Biochemistry 49:5455–5463

Wen J, Zhang H, Gross ML, Blankenship RE (2011) Native electrospray mass spectrometry reveals the nature and stoichiometry of pigments in the FMO photosynthetic antenna protein. Biochemistry 50:3502–3511

Wendling M, Pullerits T, Przyjalgowski MA, Vulto SIE, Aartsma TJ, van Grondelle R, van Amerongen H (2000) Electron–vibrational coupling in the Fenna–Matthews–Olson complex of *Prosthecochloris aestuarii* determined by temperature-dependent absorption and fluorescence line-narrowing measurements. J Phys Chem B 104:5825–5831